



## Modeling of a rail suspension system to investigate vertical vibration and effective parameters on it

Sajjad Sattari<sup>1</sup>, Mohammad Saadat<sup>1\*</sup>, Sayed Hasan Mirtalaie<sup>1</sup>, Mehdi Salehi<sup>1</sup>, Ali Soleimani<sup>1</sup>

<sup>1</sup>Department of Mechanical Engineering, Najafabad Branch, Islamic Azad University, Najafabad, Iran

### ARTICLE INFO

#### Article history:

Received: 22.04.2022

Accepted: 08.12.2022

Published: 05.03.2023

#### Keywords:

Railway

RMS acceleration

MATLAB/Simulink

Ride comfort

Suspension system

### ABSTRACT

Railways as a dimension of transportation infrastructure has been widely welcomed in developed and developing industrial countries because of the ability to carry heavy loads over long distances, more safety, less depreciation, less cost, less pollution, etc. Therefore, knowledge of the dynamic behavior of the railway is essential for designers and builders. It is very important to study the vibration and affected parameters including the specifications of the car-body, bogie, primary and secondary suspension system, track condition, rail specifications, etc., to assess the ride comfort and maintenance. This paper analyzes the effect of different parameters of a rolling stock on vertical acceleration and ride comfort by modeling a rail vehicle using MATLAB/Simulink. The First quarter of bogie suspension system was performed with step input conditions based on mathematical equations, and then the displacement, speed, and acceleration performance of the system were evaluated and validated. Finally, the effects of rolling stock parameters such as mass, and primary and secondary suspension parameters on vertical vibrations and ride comfort using root-mean-square (RMS) accelerations and Sperling comfort index were evaluated. One of the results showed that changing the parameters of the secondary suspension ( $K_1$ ,  $C_1$ ) has the greatest effect on the RMS acceleration of the car-body and ride comfort. By 50% reduction in the value of  $K_1$  and  $C_1$ , the value of ride comfort ( $W_z$ ) decreases about 14% and increases about 9%, respectively.

## 1. Introduction

The transportation section, as a prerequisite and foundation of development, has a fundamental and efficient role in the fertility of potential opportunities and talents of communities, which provides an inseparable link between various factors of growth and development through the movement of cargo and passengers. Meanwhile, rail vehicles as a dimension of transportation infrastructure have been widely welcomed in developed and developing industrial countries because of the ability to carry heavy loads over long distances, the ability to load and unload massive loads faster than other vehicles, more safety, less depreciation, less cost, less pollution and, etc.,

have been widely welcomed in developed and developing industrial countries. To maintain its competitive advantages over other industries, the rail transport industry must pay special attention to passenger safety and comfort categories. Many researchers in different countries use analytical simulation to study the dynamic properties of line structures. The advantage of this will be the replacement of time-consuming and costly physical experiments with numerical simulation studies on the issues under discussion. Various computational models have been developed in recent years and advances have been made in this field, which will be reviewed later in later sections [1-11].

Kumar et al. [4] performed numerical simulations of the vertical dynamic behavior of

\*Corresponding author

Email address: saadat@pmc.iaun.ac.ir

a rail vehicle and investigated the effect of track speed and irregularity on ride comfort. They used root-mean-square (RMS) accelerations to evaluate ride comfort. Leblebici et al. [8] studied the RMS response of a half-car model of a high-speed vehicle with random road excitations and showed that RMS vertical and pitch accelerations, suspension travel, and tire deflections are improved by active suspension design. Abood et al. [9] simulated a rail system (31-DOF) to investigate the effect of vertical secondary suspension stiffness on the ride comfort of a railway car-body. Nielsen and Igeland [10] investigated the vertical dynamic behavior of a railway bogie moving on a rail. Graa et al. [11] investigated the effect of vehicle speed and rail irregularities on ride comfort through numerical simulations (using Largege dynamics). Their model consists of 17-DOF with 4 wheelsets, 2 bogies, and a car-body; the Sperling ride index (ISO-2631) was calculated using filtered RMS acceleration to evaluate the ride comfort. Some papers [12-15] also examined the effect of rolling stock parameters such as primary and secondary suspension systems, masses, etc. on the critical speed and hunting phenomenon. For example, Serajian [12] studied the theory of branching, nonlinear lateral stability, and hunting behavior of a rail vehicle, and analyzed the effect of changing parameters on critical speeds.

Rail vehicles consist of various components, such as the car-body, bogies, springs, dampers, wheelsets, etc. Figure 1 shows the general model of a vehicle. The wagon has two bogies in the front and rear positions, each of which has four wheels in pairs and is connected by an axle. The wheelsets are connected to the bogie through the primary suspension system and the bogie is

connected to the body of the wagon through the secondary suspension system. The design of the primary suspension is to stabilize the rail vehicle in load and weight changes and the secondary suspension is to separate the main body from the line irregularities (ride comfort). Therefore, when vibrations are not maintained within a permissible level in a rail vehicle, both the comfort and safety of passengers are compromised and the service life of parts and equipment is reduced (increased maintenance costs). Therefore, undesirable vibrations in rail transportation systems reduce system performance (component failure), wagon instability, and track displacement [16-19].

Although new techniques in manufacturing and design guarantee better ride quality in rail vehicles, sometimes it is not possible to completely eliminate various track defects or ground irregularities. The dynamic behavior of a train also depends on the load and mechanical systems such as springs, dampers, etc. that interact with the wheels, the train body, and bogies. Maximum body acceleration is one of the reasons for rail vehicle ride discomfort, and accelerations are mainly due to irregularity in tracks that are transmitted to the body through the driving parts. To achieve ride comfort, these accelerations must be suppressed. To improve ride comfort, it is important to better understand the route parameters that affect riding behavior [9-11, 16-18]. It requires the analysis of vehicle parameters in riding behavior and provides important information about the impact of each parameter on the acceleration response to rail vehicle designers. This information can also be used to achieve the right combination of design parameters, which can help maintain maximum acceleration peaks in the standard comfort range,

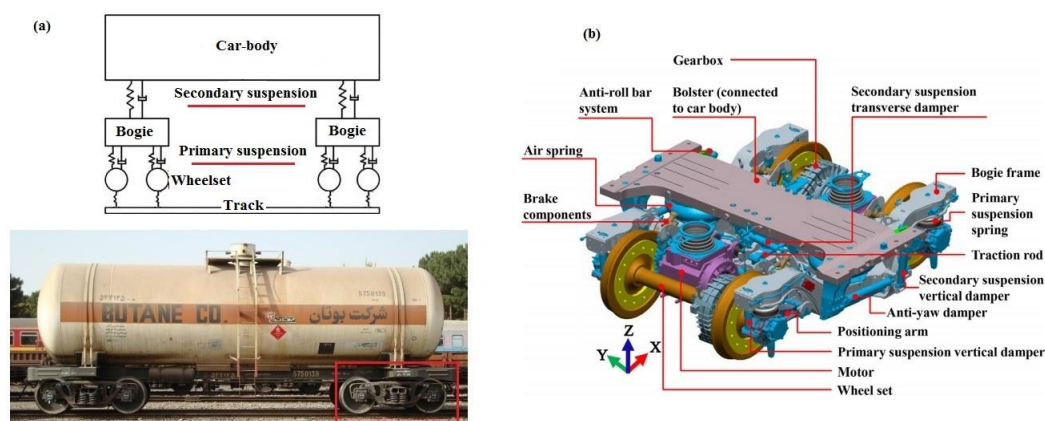


Figure 1. Schematic of (a) a railway system and freight wagon, and (b) detail of the bogie [19].

which improves the ride. Therefore, the analysis of rail vehicle parameters that affect ride behavior simulates the real dynamics of the rail vehicle system using efficient and reliable simulation software and provides better input for understanding and designing low-cost rail vehicles.

This paper discusses the effect of some rail vehicle parameters such as body mass, bogie mass, wheel mass, primary and secondary suspension systems, and the wheel-rail contact stiffness on vertical accelerations (body, bogie, and wheel), and ride comfort. The analysis was performed by modeling and simulating a rail vehicle using the Simulink environment of MATLAB software. RMS accelerations were compared for evaluation and the relevant equations were used to evaluate the ride comfort.

## 2. Evaluation criteria (RMS acceleration and comfort index)

The rail vehicle consists of a locomotive, car-body, bogie, primary and secondary suspension, and wheelsets. As the train travels along the track, it forms an interaction system with the rail track. The dynamic analysis of such a system will mainly cover the following issues: (a) check the safety of trains along the tracks, (b) evaluate the existing tracks, etc., and (c) determine the quality of the trains' riding quality [20]. Ride comfort is affected by two general factors (based on physical factors); some due to the movement of the rail vehicle, such as vibrations and noise, while others due to the environmental conditions inside the rail vehicle such as temperature,

humidity, and air speed, lighting or interior accessories and decoration (for example shape and location of seats). Among all the factors affecting comfort, the vibrations of rail vehicles are considered the main factor in determining ride comfort [21-23]. Various evaluation methods for ride comfort have been developed with selective applicability depending on the traffic type, such as urban, suburban, underground, long-distance, etc. The most commonly accepted principles of vibration perception evaluation are laid out in the international standard ISO 2631 [24-26], the evaluation criteria based on the Sperling index [27-28], and the standard UIC 513 [29] proposed by the international union of railways and included in the European standard EN 12299 [30]. The ride index Wz method was brought to Germany by Sperling in the mid-20th century, and it provides the most well-known evaluation method for the ride comfort and ride quality of railway vehicles. It introduces the concept of the ride comfort index (Wz ride comfort index) [17, 31]. The sperling index was derived using the results obtained from the model. The acceleration of the car-body in the time domain ( $\ddot{Z}_c(t)$ ) is computed. The vertical car-body accelerations are transformed into the frequency domain through the Fast Fourier Transform (FFT) of ( $\ddot{Z}_c(t)$ ) as indicated under [32]:

$$\{\ddot{Z}_c(f)\} = \{FFT(\ddot{Z}_c(t))\} \quad (1)$$

Subsequently, the weighted car-body vertical acceleration in the frequency domain  $\{\ddot{Z}_c(f)\}_w$  is obtained based on Sperling frequency filter as under [32-33]:

Table 1. Sperling's comfort index and vehicle ride quality index [32, 35]

W <sub>z</sub> Ride comfort		W <sub>z</sub> Vehicle ride	
1.0	Just noticeable	1.0	Very good
2.0	Clearly noticeable	2.0	Good
2.5	More pronounced but not unpleasant	3.0	Satisfactory
3.0	Strong, irregular, but still tolerable	4.0	Acceptable for running
3.25	Very irregular	4.5	Not acceptable for running
3.5	Extremely irregular, unpleasant, annoying; prolonged exposure intolerable	5.0	Dangerous
4.0	Extremely unpleasant; prolonged exposure harmful		

$$\{\ddot{Z}_c(f)\}_w = \{B(f)\} \cdot \{\ddot{Z}_c(f)\} \quad (2)$$

where

$$\{B(f)\} = \left\{ 0.588 \left[ \frac{1.911f^2 + (0.25f^2)^2}{(1 - 0.277f^2)^2 + (1.563f - 0.0368f^3)^2} \right]^{0.5} \right\} \quad (3)$$

In equation (3),  $f$  represents the frequency (Hz). The weighted vertical acceleration in the time domain is derived through Inverse Fourier Transform (IFT) [32, 34] of  $\{\ddot{Z}_c(f)\}_w$  as under:

$$\{\ddot{Z}_c(t)\}_w = IFT(\{\ddot{Z}_c(f)\}_w) \quad (4)$$

Finally, Sperling Index ( $W_z$ ) is obtained using equation (5) in which  $a_{rms}$  is the RMS of  $\{\ddot{Z}_c(t)\}_w$  [32-33]:

$$W_z = 4.42(a_{rms})^{0.3} \quad (5)$$

To evaluate the ride quality and ride comfort of a railway vehicle, the ride index ( $W_z$ ) was introduced by Sperling. Sperling's comfort level characterization is given in Table 1. Therefore, the effects of rail vehicle parameters on vertical vibrations and ride comfort using RMS accelerations (acceleration-time curves) and Sperling comfort index were evaluated and comprehensive explanations are provided in the following sections.

### 3. Modeling

#### 3.1. Modeling method

In this study, first, a suspension system (ICF bogie) was simulated by MATLAB/Simulink according to the research of Karthik et al. [36]. Figure 2 shows the model of the rail vehicle in this study (a quarter is modeled). The component specifications are characterized as car-body with the mass of  $M_1$ , the body of bogie with the mass of  $M_2$ , and the wheel with the mass of  $M_3$  and the displacements of  $U_1$ ,  $U_2$ , and,  $U_3$  for body, bogie, and wheel respectively (the track input is represented by  $t$ ). Primary and secondary suspension systems include springs and dampers with  $K_2$ ,  $C_2$ ,  $K_1$ , and  $C_1$ , and  $K_3$  is rail-wheel contact stiffness. In the study paper [36], the performance of a rail suspension system was simulated using MATLAB/Simulink under step input conditions, and displacement, speed, and acceleration diagrams were extracted over time. The simulations performed in this work neglect any track irregularities and assume the new wheel to be rolling on a smooth, level, and tangent track [15, 36-38].

The mathematical equations with 3-DOF are developed for the model shown in Figure 2. By considering the free body diagrams of all the masses, Newton's second law of motion is applied. The corresponding equations are:

$$M_1 \ddot{U}_1 = -C_1(\dot{U}_1 - \dot{U}_2) - K_1(U_1 - U_2) \quad (6)$$

$$M_2 \ddot{U}_2 = -C_1(\dot{U}_2 - \dot{U}_1) - C_2(\dot{U}_2 - \dot{U}_3) - K_1(U_2 - U_1) - K_2(U_2 - U_3) \quad (7)$$

$$M_3 \ddot{U}_3 = -C_2(\dot{U}_3 - \dot{U}_2) - K_2(U_3 - U_2) - K_3(U_3 - t) \quad (8)$$

The state variable form of the above equations is given by,

$$\dot{Y} = AY + BZ \quad (9)$$

where

$$\dot{Y} = \begin{bmatrix} \dot{Y}_1 \\ \dot{Y}_2 \\ \dot{Y}_3 \\ \dot{Y}_4 \\ \dot{Y}_5 \\ \dot{Y}_6 \end{bmatrix}, Y = \begin{bmatrix} Y_1 \\ Y_2 \\ Y_3 \\ Y_4 \\ Y_5 \\ Y_6 \end{bmatrix}, Z = \begin{bmatrix} 0 \\ 0 \\ 0 \\ 0 \\ 0 \\ t \end{bmatrix} \quad (10)$$

$$B = \begin{bmatrix} 0 & 0 & 0 & 0 & 0 & 0 \\ 0 & 0 & 0 & 0 & 0 & 0 \\ 0 & 0 & 0 & 0 & 0 & 0 \\ 0 & 0 & 0 & 0 & 0 & 0 \\ 0 & 0 & 0 & 0 & 0 & 0 \\ 0 & 0 & 0 & 0 & 0 & \frac{K_3}{M_3} \end{bmatrix} \quad (11)$$

$$A = \begin{bmatrix} 0 & 0 & 0 & 1 & 0 & 0 \\ 0 & 0 & 0 & 0 & 1 & 0 \\ 0 & 0 & 0 & 0 & 0 & 1 \\ -\frac{K_1}{M_1} & \frac{K_1}{M_1} & 0 & -\frac{C_1}{M_1} & \frac{C_1}{M_1} & 0 \\ \frac{K_1}{M_2} & -\frac{(K_1+K_2)}{M_2} & \frac{K_2}{M_2} & \frac{C_1}{M_2} & -\frac{(C_1+C_2)}{M_2} & \frac{C_2}{M_2} \\ 0 & \frac{K_2}{M_3} & -\frac{(K_2+K_3)}{M_3} & 0 & \frac{C_2}{M_3} & -\frac{C_2}{M_3} \end{bmatrix} \quad (12)$$

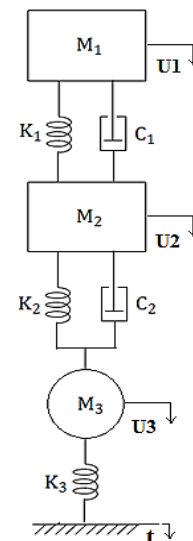


Figure 2. Dynamic suspension model for simulation.

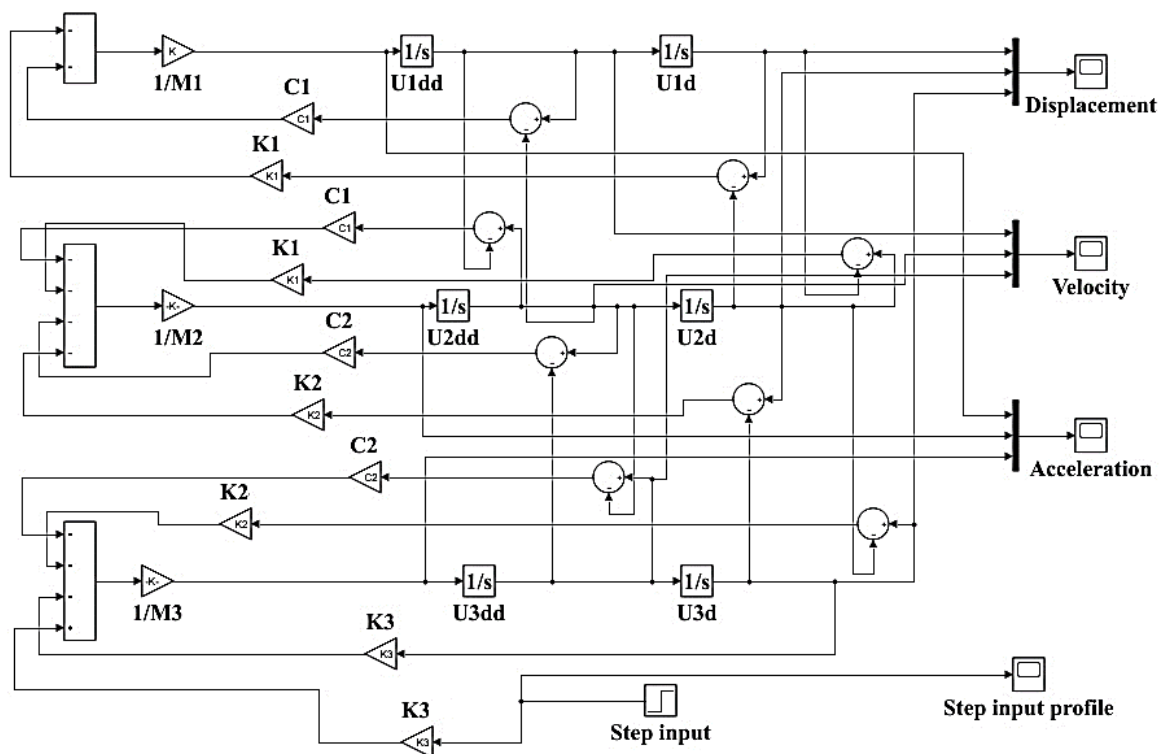


Figure 3. MATLAB/Simulink model.

The equivalent Simulink model of the system is created according to the equations (6), (7), and (8) as shown in Figure 3.

In the present article, according to Table 2 [20], the effect of each of the mentioned parameters on the vertical acceleration of the body, bogie, and wheel has been investigated. Also, according to the sperling index (equation 5), the ride comfort level has been calculated.

In this study, any curve is not considered and it is limited to straight lines, which means that there is only vertical interaction between the vehicle and the track. Therefore, only the vertical vibration of the vehicle in the simulation was considered. The sperling index (one of the most widely used indexes in railway research [39-41]) was used to provide the level of ride comfort.

Table 2. Body, bogie, and wheel parameters.

Parameters	Symbol	Values
Mass of the car body	$M_1$	3500 (kg)
Mass of the bogie	$M_2$	250 (kg)
Mass of the wheel	$M_3$	350 (kg)
Secondary spring stiffness	$K_1$	$0.14 \times 10^6$ (N/m)
Primary spring stiffness	$K_2$	$1.26 \times 10^6$ (N/m)
Wheel-rail contact stiffness (assumption)	$K_3$	$10^5$ (N/m)
Secondary damping coefficient	$C_1$	$8.87 \times 10^3$ (Ns/m)
Primary damping coefficient	$C_2$	$7.1 \times 10^3$ (Ns/m)

The effectiveness and accuracy of this index have been demonstrated in the available literature. It is noteworthy that the selected ranges and values for  $M_1$ ,  $M_2$ ,  $M_3$ ,  $K_1$ ,  $K_2$ ,  $K_3$ ,  $C_1$ , and  $C_2$  have been extracted from different sources [4, 8, 9, 11, 17, 20, 35, 42-44].

### 3.2. Validation

Figure 4 shows the restimulation results of [36] with current research. The results are in

complete agreement with the reference. From Figure 4(b), the result shows that the major displacement of the body and the bogie frame is related to the long sitting time and the wheel sitting time is very small compared to the body and the bogie frame. From Figure 4(c), the result shows that a maximum speed is recorded for the system and the time required for the body and bogie to settle is high compared to the wheel. In Figure 4(d), the maximum acceleration is

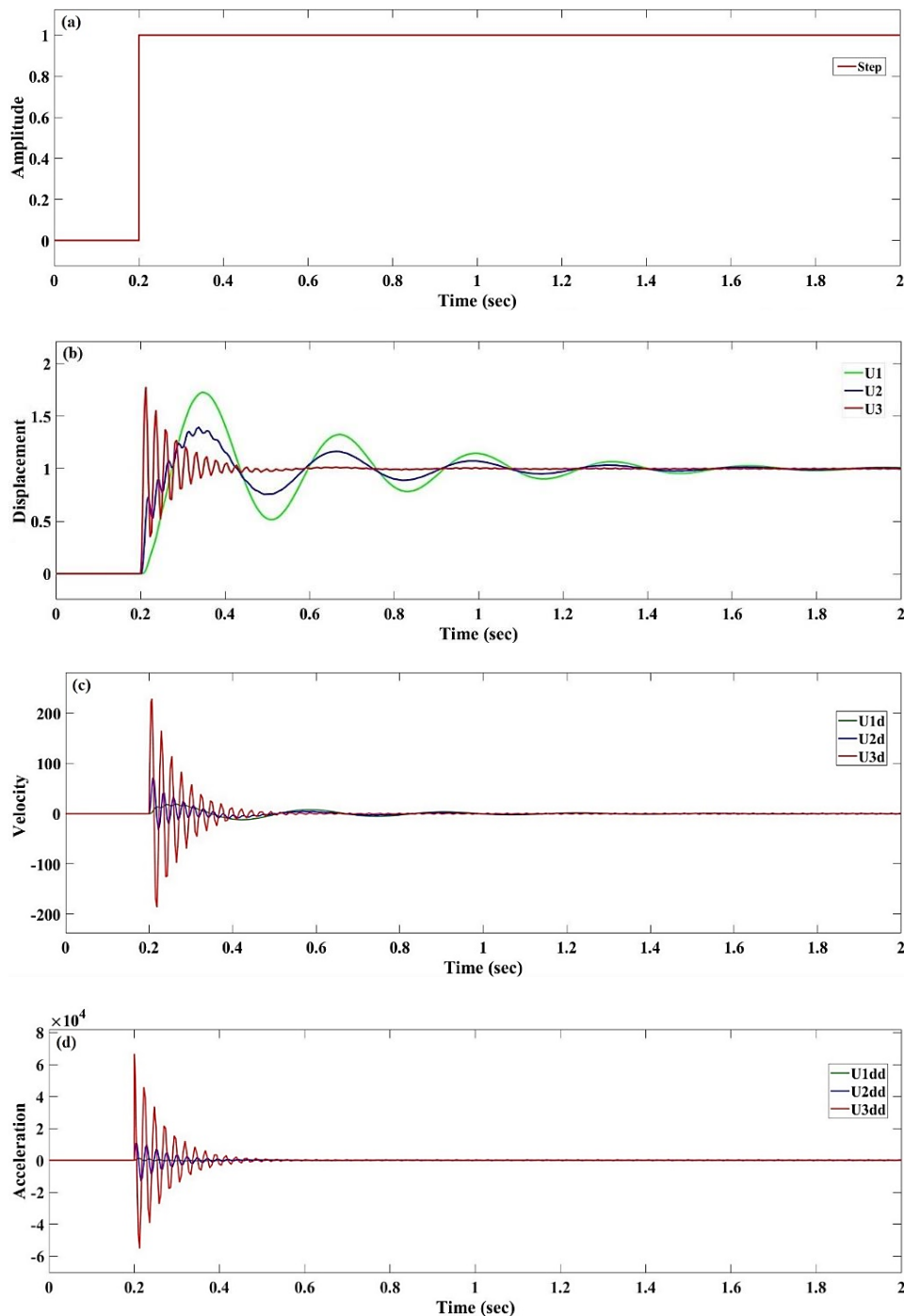


Figure 1. (a) Step input signal, (b) Displacement-time, (c) Speed-time, (d) Acceleration-time.



recorded for the wheel compared to the body and bogie, but the settling time is the same for all accelerated mass components.

#### 4. Investigation and discussion about the effect of different operational parameters

Figure 5 indicates acceleration-time curves for the body, bogie, and wheel of the rail vehicle. The input values in this diagram are given following Table 2. After extracting the diagram according to the mentioned parameters, the RMS acceleration values for the body, bogie, and wheel and the comfort parameter of the body can be seen in Table 3. According to the comfort index (Table 1), the ride comfort status is in a discomfort state and we should try to improve this index by changing the parameters. In the following sections, the effect of different parameters is examined.

#### 4.1. Effects of variation in the value of $K_1$

Figure 6 illustrates acceleration-time curves with different values of  $K_1$  for the body, bogie, and wheel. As can be seen, with increasing the values of  $K_1$ , the amount of acceleration on the body increases, but the changes in acceleration on the bogie and the wheel are very small. Figure 7 shows the RMS acceleration values and comfort parameters of the body. It should be noted that the body comfort for  $K_1=0.0035 \times 10^6$  (N/m) is in a relatively good position (more pronounced but not unpleasant). Abood et al. [9] presented a mathematical model of a train with two bogies and two wheelsets in each bogie with 31-DOF and investigated the influence of vertical secondary suspension spring stiffness on the ride comfort of a railway car-body at speeds below and at critical hunting speed. Their results showed that high magnitudes of vertical

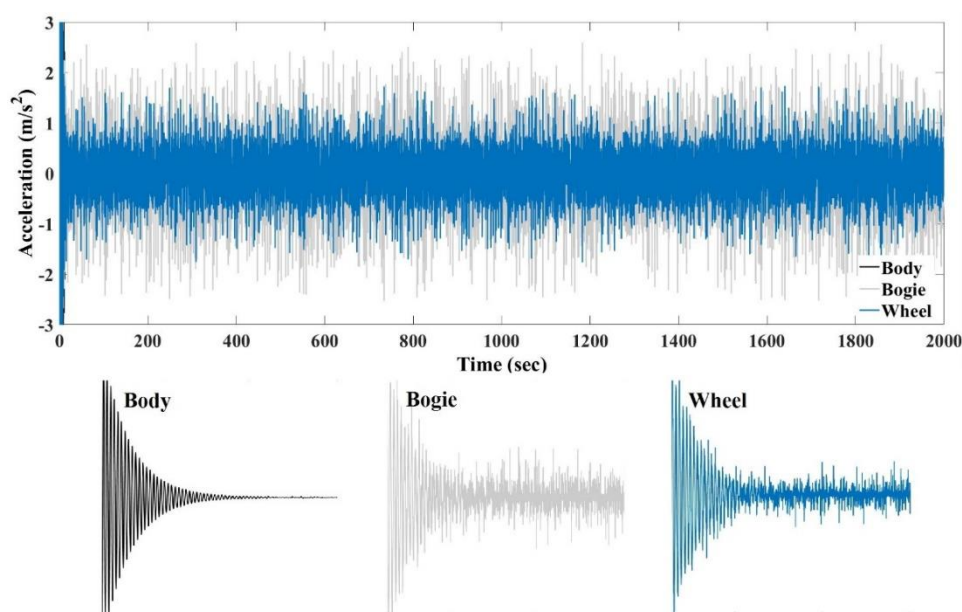


Figure 2. Acceleration-time curves for the body, bogie and wheel according to Table 2.

Table 2. Values of the RMS accelerations ( $a_{RMS}$ ).

$(a_{RMS})_{Body}$	$(a_{RMS})_{Bogie}$	$(a_{RMS})_{Wheel}$	$(W_z)_{Body}$
0.47	1.37	2.47	3.52

secondary spring stiffness suspension introduce undesirable roll and yaw dynamic responses which affect ride comfort at critical hunting velocity by modeling a rail system that is consistent with the results of the current article. Or in another article, Wu et al. [18] developed a coupled track-train-seat-human model with

lateral, vertical, and roll vibrations to investigate the ride comfort (by the total equivalent acceleration defined according to ISO 2631-1) of high-speed trains. Their studies stated that an increase in the vertical stiffness of the second suspension seemed to cause a slight increase in the total equivalent acceleration.

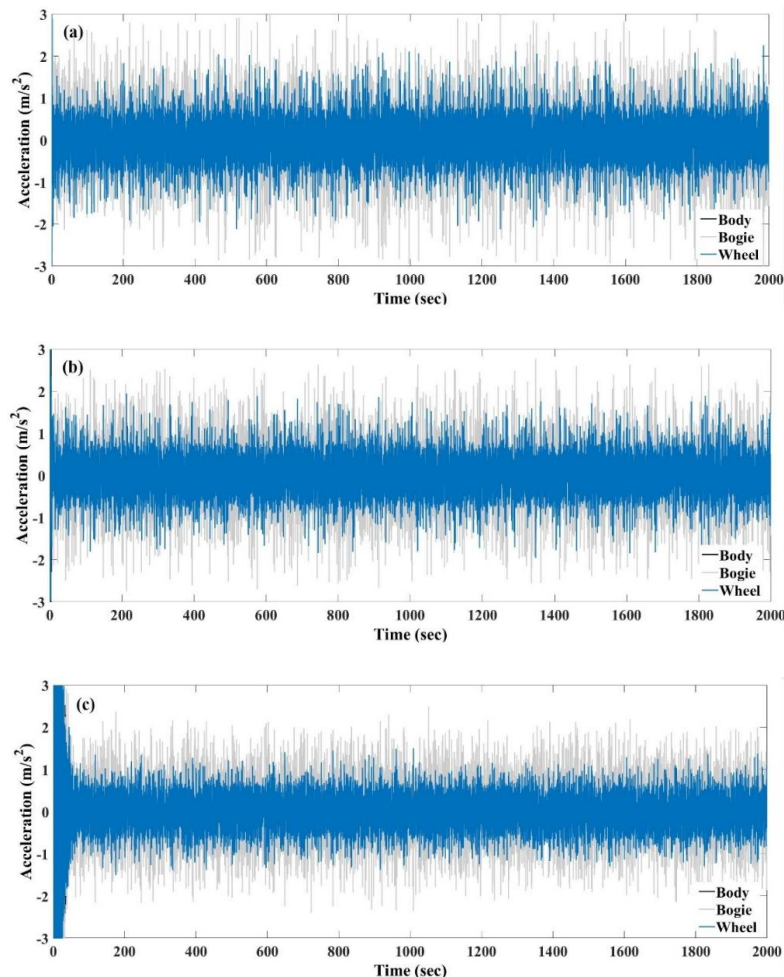


Figure 3. Acceleration-time curves for different values: (a)  $K_1=0.0035 \times 10^6$  (N/m), (b)  $K_1=0.07 \times 10^6$  (N/m) and (c)  $K_1=0.28 \times 10^6$  (N/m).

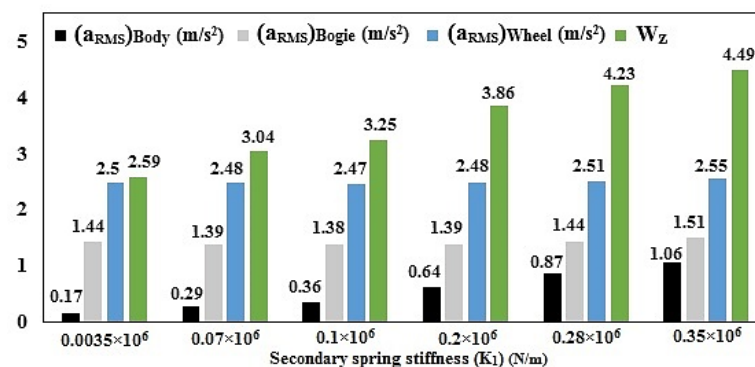


Figure 4. The RMS accelerations and  $(W_z)_{Body}$  for different values of  $K_1$ .



#### 4.2. Effects of variation in the value of $K_2$

Figure 8 shows acceleration-time curves with different values of  $K_2$  for the body, bogie, and wheel. Also, the values of RMS acceleration and ride comfort are presented in Figure 9. As can be seen, changes in the value of  $K_2$  have little effect on the acceleration of the body, bogie, and wheel, and of course, there is no noticeable change in ride comfort. For example, with a decrease of 50%, 77%, and 88% of the value of

$K_2$  from the original value, the body RMS acceleration is decreased by 0%, 6%, and 21%, respectively, and with an increase of 43%, 100% and 217% of the value of  $K_2$  from the original value, the body RMS acceleration changes 0%, 2% and 2% respectively that can be ignored. It should also be noted that changes in the value of  $K_2$  had the greatest influence on bogie acceleration and with increasing the value of  $K_2$ , bogie acceleration is increased.

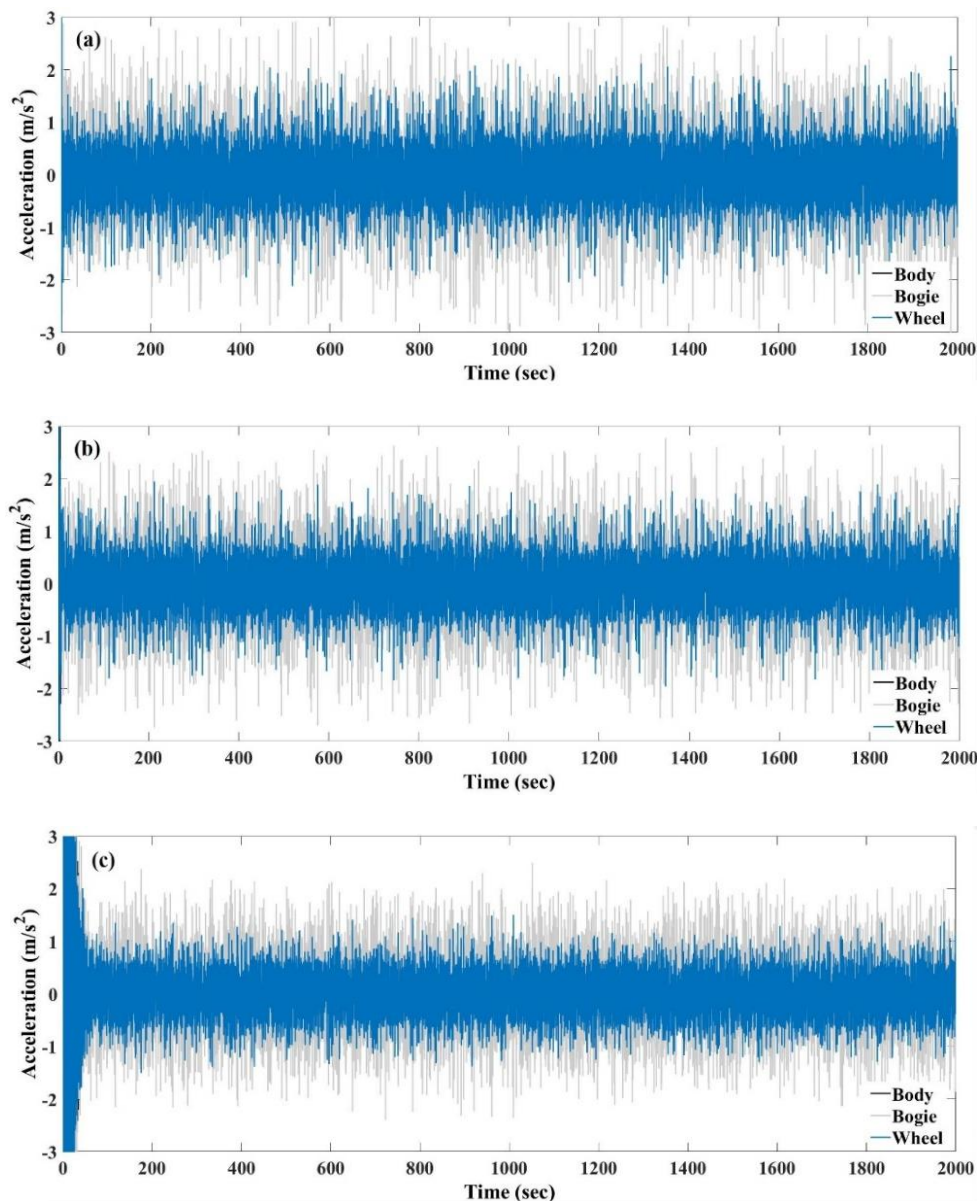
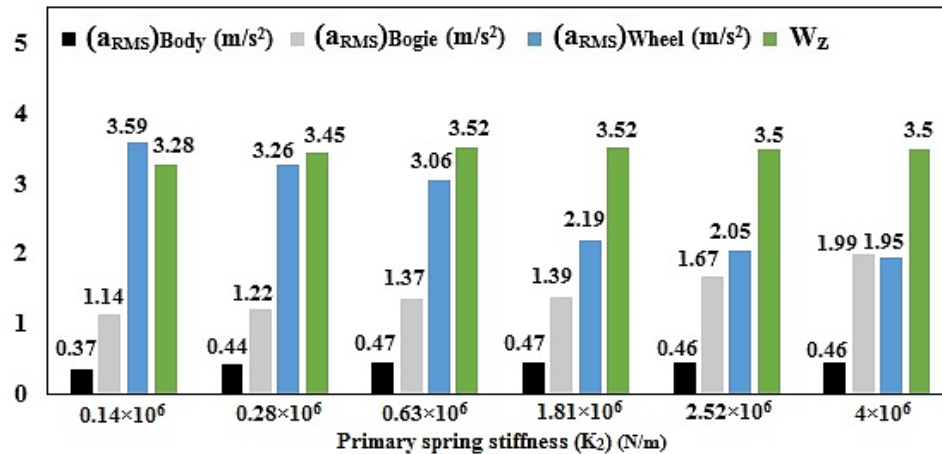


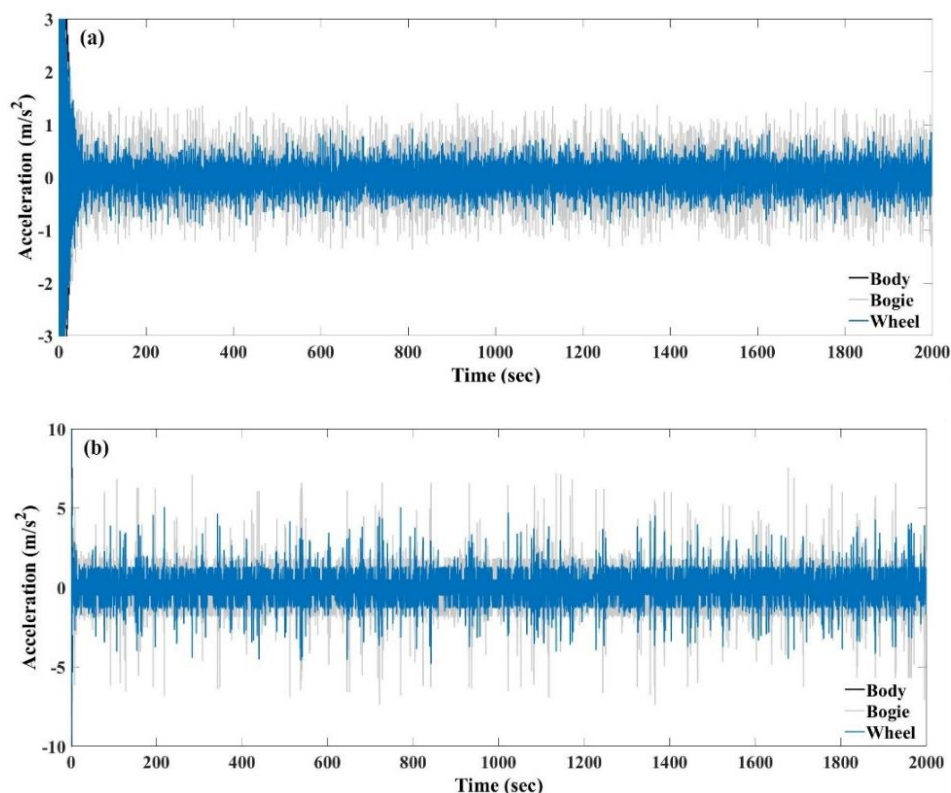
Figure 8. Acceleration-time curves for different values: (a)  $K_2=0.28 \times 10^6$  (N/m), (b)  $K_2=0.63 \times 10^6$  (N/m) and (c)  $K_2=1.81 \times 10^6$  (N/m).


 Figure 9. The RMS accelerations and  $(W_z)_{Body}$  for different values of  $K_2$ .

#### 4.3. Effects of variation in the value of $K_3$

Figure 10 shows acceleration-time curves with different values of  $K_3$  for the body, bogie, and wheel. As can be seen in Figure 11, with increasing the value of  $K_3$ , the accelerations of the body, bogie, and wheel are increased and, of course, the quality of comfort is decreased. It should be noted that  $K_3$  is more dependent on changes and with the smallest changes, the

accelerations will change significantly. The effects of vehicle speed, bridge flexibility, and random or non-random road irregularities on ride comfort have been extensively investigated by Koç et al. [45]. One of their results showed that increasing the value of  $K_3$  increased the value of body RMS acceleration, which is consistent with the current article.


 Figure 5. Acceleration-time curves for different values: (a)  $K_3=5 \times 10^4$  (N/m) and (b)  $K_3=4 \times 10^5$  (N/m).

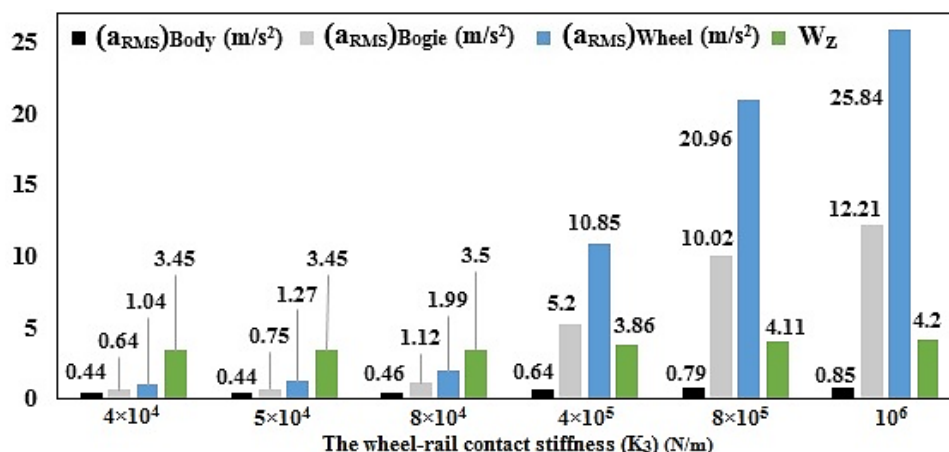


Figure 6. The RMS accelerations and  $(W_z)_{Body}$  for different values of  $K_3$ .

#### 4.4. Effects of variation in the value of $C_1$

Figure 12 shows acceleration-time curves with different values of  $C_1$  for the body, bogie, and wheel. According to Figure 13, it can be concluded that the changes of  $C_1$  have the greatest effect on the acceleration of the body, and with increasing the value of  $C_1$ , the acceleration of the body decreases significantly. It is also noteworthy that with increasing the value of  $C_1$ , the RMS accelerations of the bogie and wheel are decreased. Wu et al. [18] also showed that the total equivalent acceleration was reduced obviously in the whole speed range by increasing the car-body damping. Therefore, increasing car-body damping is an effective way to suppress the elastic vibration of the car-body, thereby improving ride comfort.

#### 4.5. Effects of variation in the value of $C_2$

Figure 14 shows acceleration-time curves with different values of  $C_2$  for the body, bogie, and wheel. By observing the values of RMS accelerations in Figure 15, it can be concluded that with increasing the value of  $C_2$ , the accelerations of the body, bogie, and wheel have decreased. Also, changes in RMS acceleration of the body and ride comfort were negligible. It should be noted that according to reference [20], an excessive increase in the value of  $C_2$  ( $39.2 \times 10^3$  (Ns/m)) causes a significant increase in the values of acceleration and vibration and is not suitable for design. Also, it should be noted that Wu et al. [18] showed that the vertical stiffness and damping had more influence on ride comfort than the fore-and-aft and lateral ones because the vertical stiffness and damping

had a significant influence on the vertical accelerations at the feet and at the seat pan that was of great significance to ride comfort, while the effects of lateral and fore-and-aft stiffness and damping of the two suspensions on the vertical vibration were small.

#### 4.6. Effects of variation in the value of $M_1$

Figure 16 shows acceleration-time curves with different values of  $M_1$  for the body, bogie, and wheel. Increasing the mass of the vehicle body ( $M_1$ ) reduces the acceleration and vibration on the body and decreasing it increases the acceleration and vibration of the body. Increasing or decreasing the value of  $M_1$  in the area of this study has little effect on the acceleration of the bogie and wheel (Figure 17). It is noteworthy that the amount of  $W_z$  has significantly decreased with increasing body mass and ride comfort has improved. Sharma [46] investigated the effect of rail vehicle parameters on vertical and lateral comfort behavior. It was seen from parametric analysis that car body mass, secondary suspension vertical damping, primary suspension vertical damping, and wheel base are the most sensitive parameters influencing vertical ride. One of his results showed that an increase in body mass improves vertical and lateral comfort at all frequencies, which is consistent with the current paper.

#### 4.7. Effects of variation in the value of $M_2$

Figure 18 shows acceleration-time curves with different values of  $M_2$  for the body, bogie, and wheel. Increasing the mass of the bogie ( $M_2$ ) reduces the acceleration and vibration on the bogie and decreasing it increases the

acceleration and vibration of the bogie. Increasing or decreasing the value of  $M_2$  in the area of this study has little effect on the acceleration of the body and wheel (Figure 19).

#### 4.8. Effects of variation in the value of $M_3$

Figure 20 shows acceleration-time curves with different values of  $M_3$  for the body, bogie, and wheel. Increasing the mass of the wheel ( $M_3$ ) reduces the acceleration and vibration of the wheel and decreasing it increases the acceleration and vibration of the wheel. For

example, with a decrease of 28%, 57%, and 71% of the value of  $M_3$  from the original value, the wheel RMS acceleration is increased by 26%, 80%, and 168%, respectively, and with an increase of 21%, 71%, and 157% of the value of  $M_3$  from the original value, the wheel RMS acceleration is decreased by 13%, 31%, and 50%, respectively (Figure 21). Increasing or decreasing the value of  $M_3$  in the area of this study has little effect on the acceleration of the body and bogie.

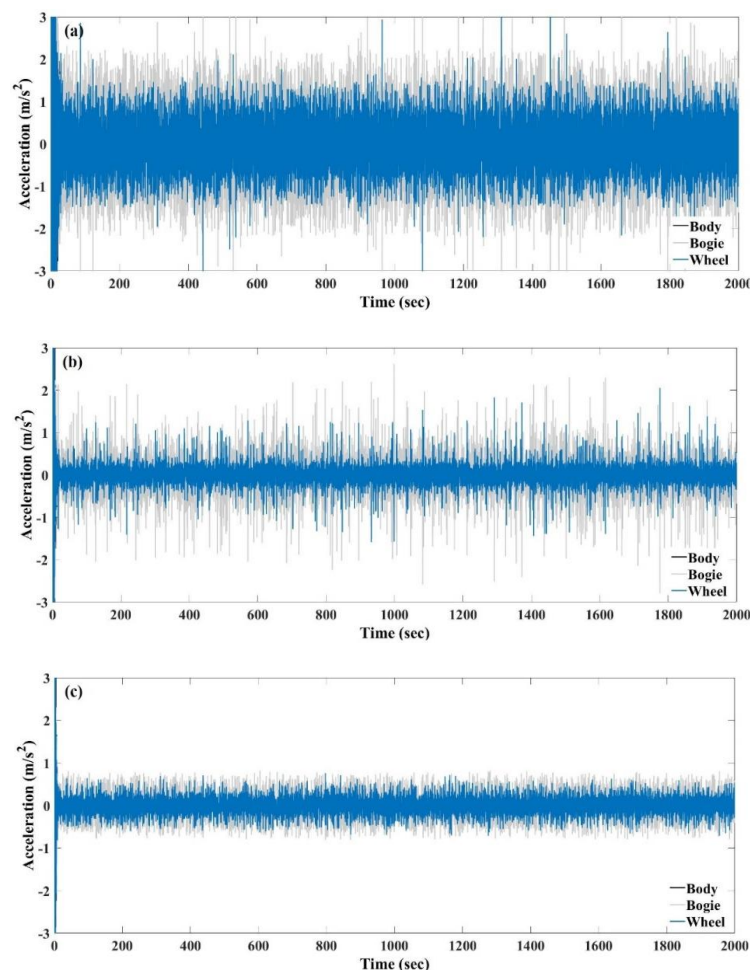


Figure 7. Acceleration-time curves for different values: (a)  $C_1=4.43 \times 10^3$  (Ns/m), (b)  $C_1=14 \times 10^3$  (Ns/m) and (c)  $C_1=22.6 \times 10^3$  (Ns/m).

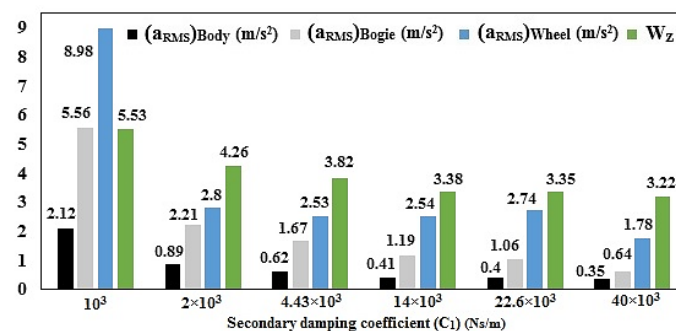


Figure 8. The RMS accelerations and  $(W_z)_{Body}$  for different values of  $C_1$ .



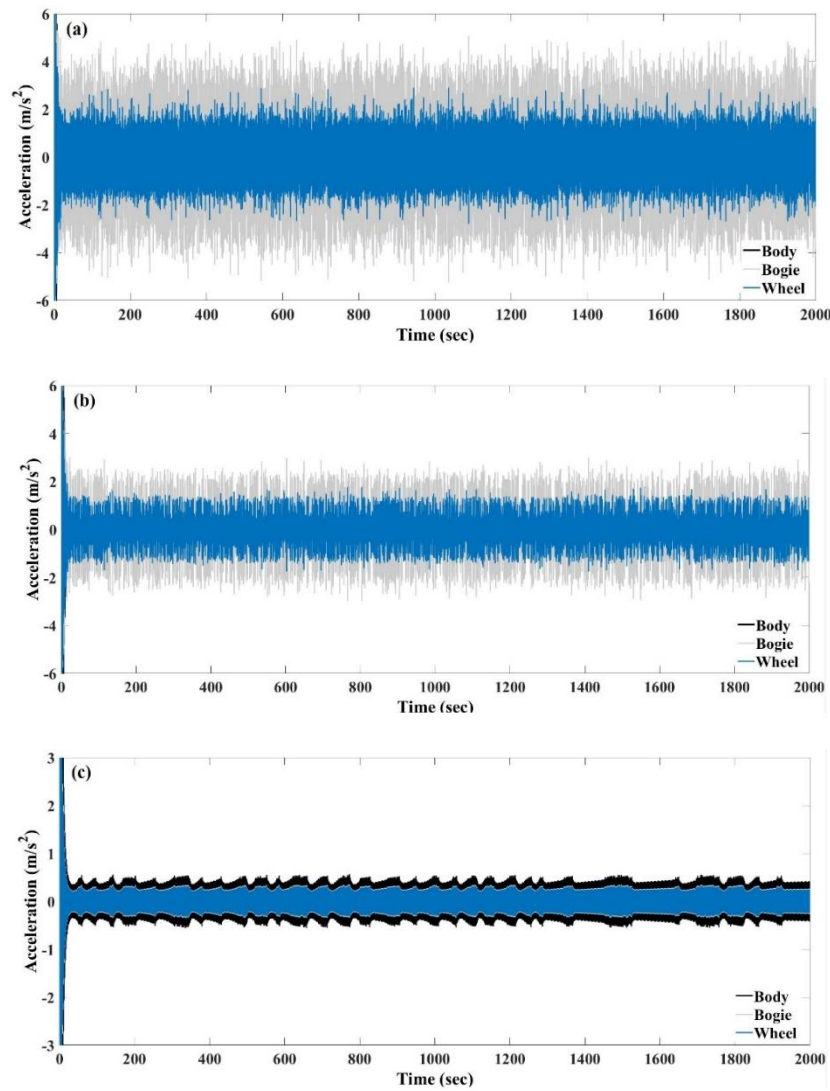


Figure 9. Acceleration-time curves for different values: (a)  $C_2=1.14 \times 10^3$  (Ns/m), (b)  $C_2=3.7 \times 10^3$  (Ns/m) and (c)  $C_2=39.2 \times 10^3$  (Ns/m).

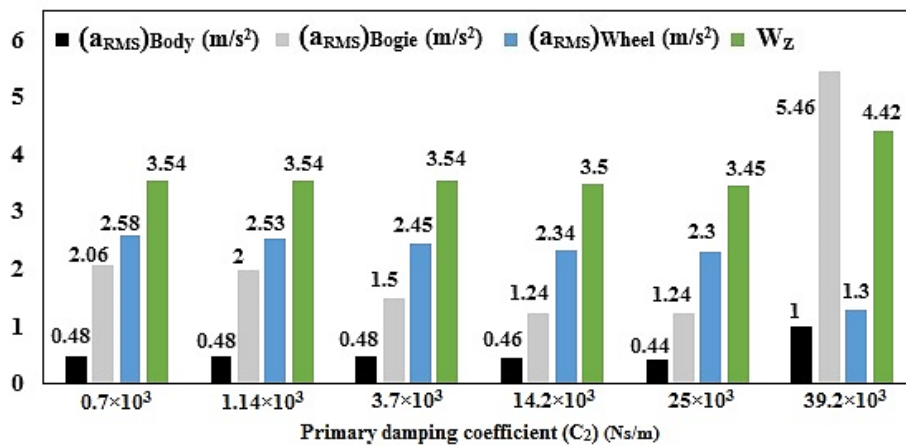


Figure 10. The RMS accelerations and  $(W_z)_{Body}$  for different values of  $C_2$ .



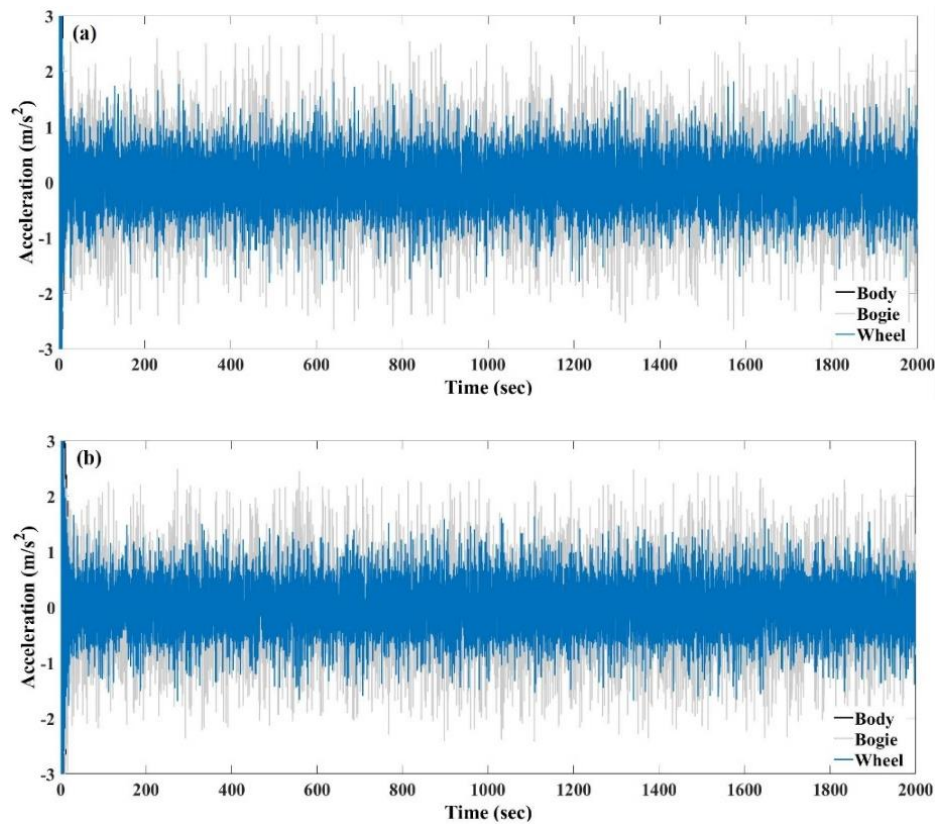


Figure 11. Acceleration-time curves for different values: (a)  $M_1=2000$  (kg) and (b)  $M_1=6500$  (kg).

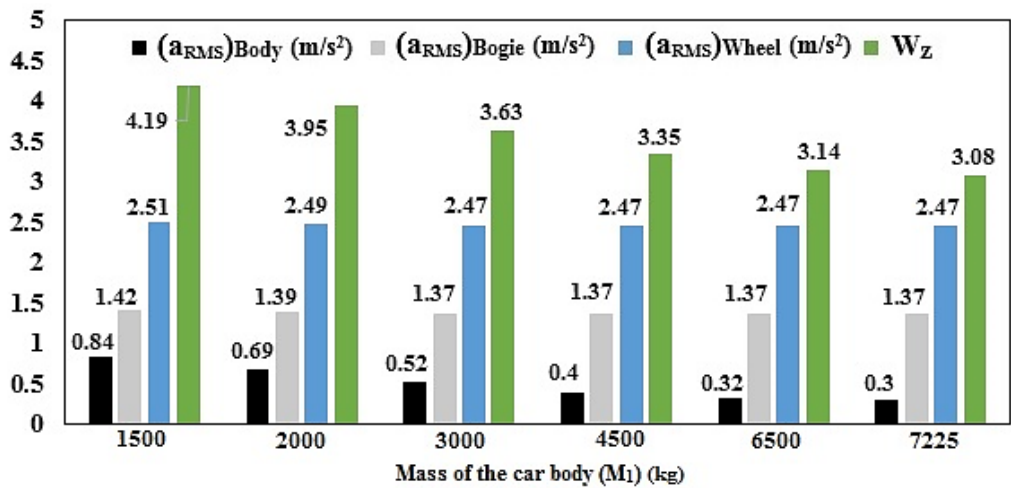


Figure 12. The RMS accelerations and  $(W_z)_{Body}$  for different values of  $M_1$ .

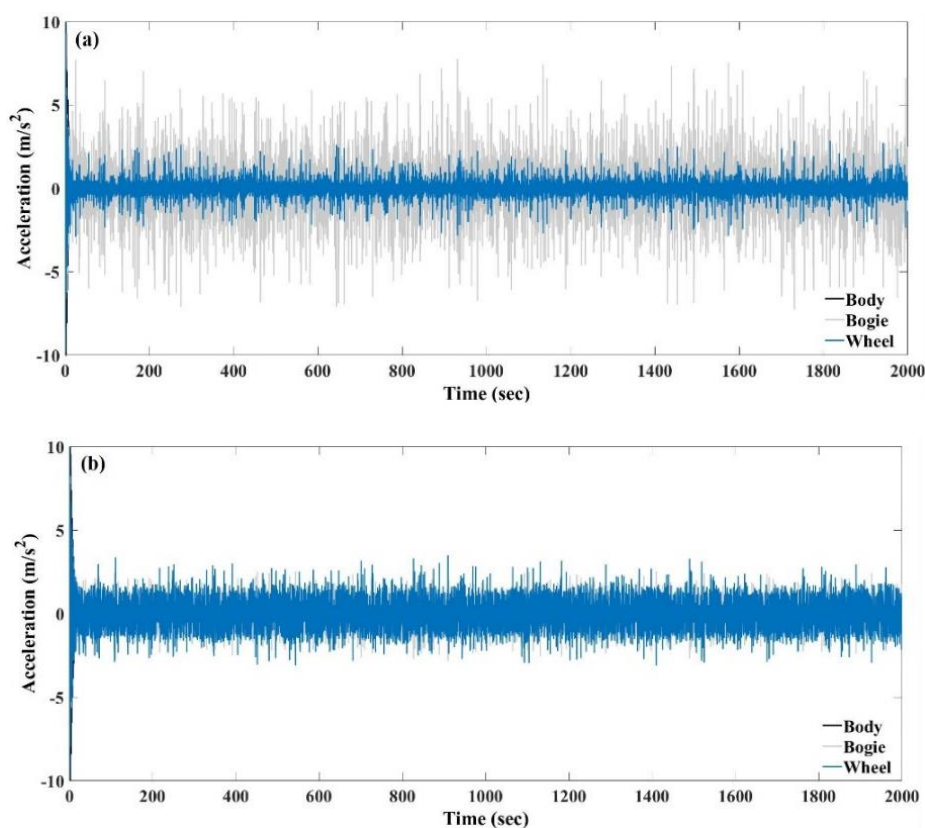


Figure 13. Acceleration-time curves for different values: (a)  $M_2=150$  (kg) and (b)  $M_2=450$  (kg).

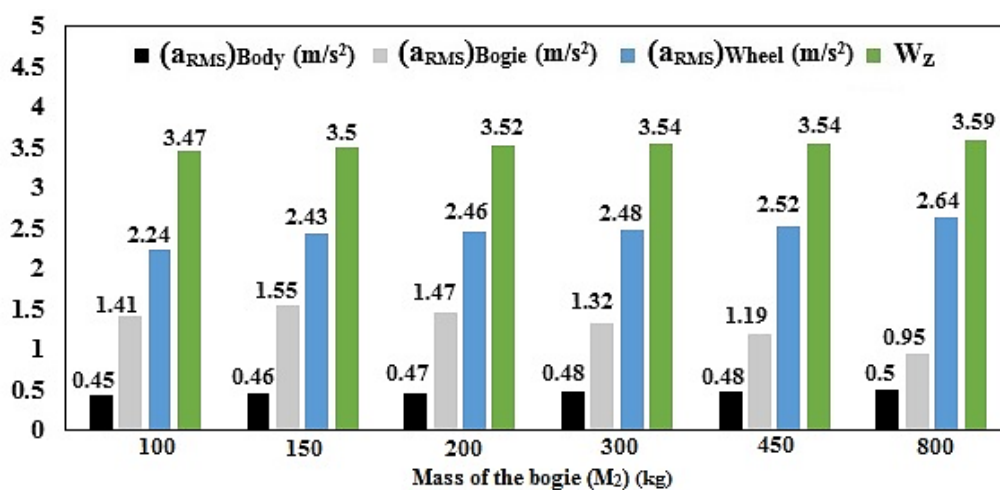


Figure 14. The RMS accelerations and  $(W_z)_{Body}$  for different values of  $M_2$ .

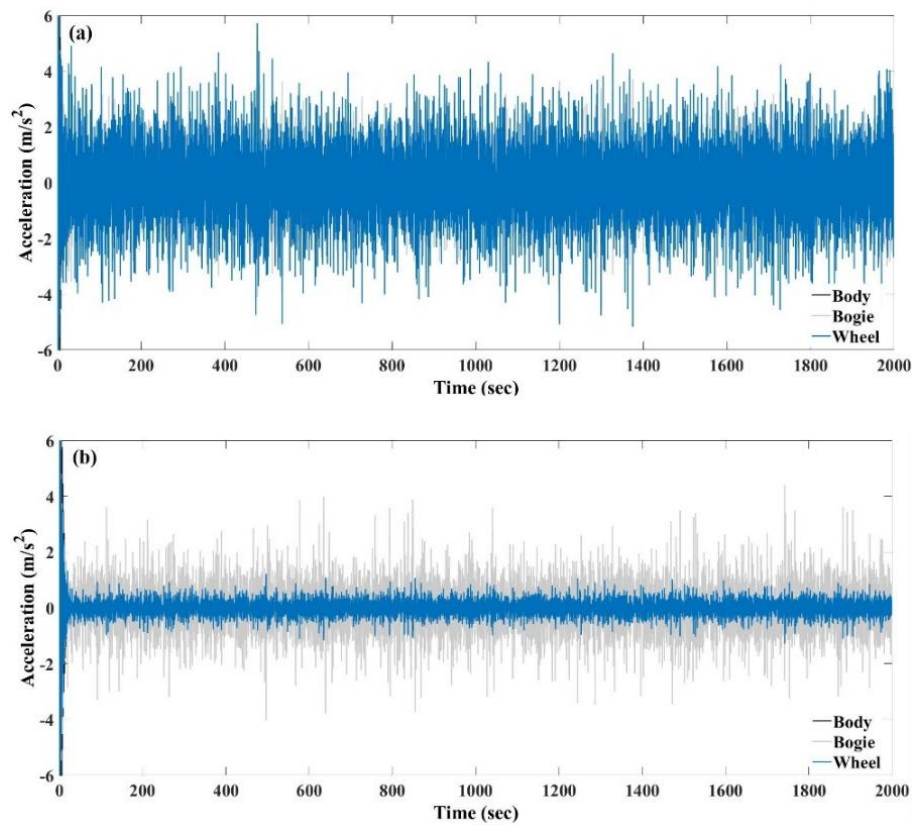


Figure 15. Acceleration-time curves for different values: (a)  $M_3=150$  (kg) and (b)  $M_3=600$  (kg).

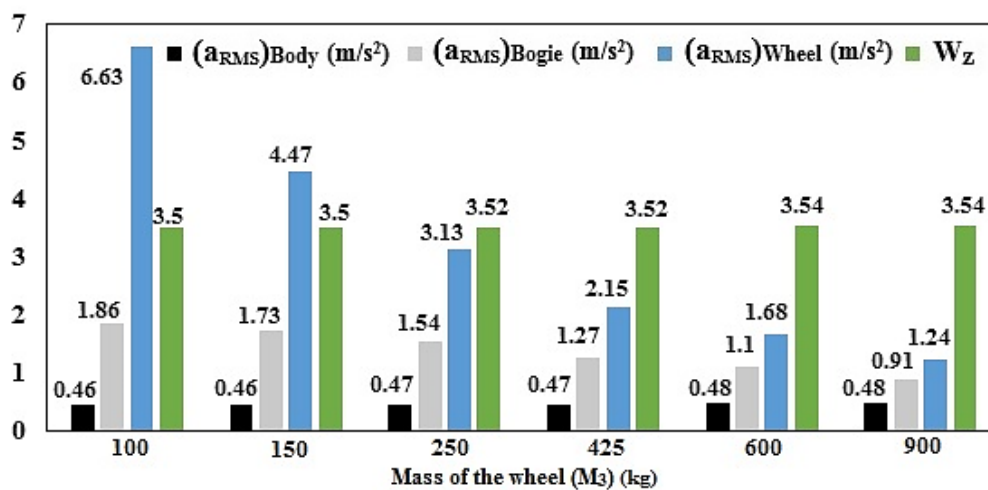


Figure 16. The RMS accelerations and  $(W_z)_{Body}$  for different values of  $M_3$ .

## 5. Conclusions

In this study, after checking the accuracy of the simulation method by comparing the results with the mentioned article, the simulation was performed again and the effect of different parameters was investigated. The important results of this research are as follows:

- By increasing the value of  $K_1$ , the body RMS acceleration values are increased, but the change in RMS accelerations on the bogie and wheel is very small. With a 50% reduction in the value of  $K_1$ , the value of ride comfort ( $W_z$ ) decreases by about 14%.

- Changes in the value of  $K_2$  have minor effects on the acceleration of the body, bogie, and wheel, and of course, there is no significant change in ride comfort. Also, changes in the value of  $K_2$  had the greatest effect on the acceleration of the bogie. For example, with a decrease of 50%, 77%, and 88% of the value of  $K_2$  from the original value, the body RMS acceleration is decreased by 0%, 6%, and 21%, respectively, and with an increase of 43%, 100% and 217% of the value of  $K_2$  from the original value, the body RMS acceleration changes 0%, 2% and 2% respectively that can be ignored.

- By increasing the value of  $K_3$ , the acceleration of the body, bogie, and wheel are increased and of course, the quality of comfort is decreased. It should be noted that  $K_3$  is more dependent on values and with the smallest changes, the accelerations will change significantly.

- Changes in  $C_1$  have the greatest effect on the acceleration of the body and with increasing the value of  $K_1$ , the acceleration of the body is decreased significantly. With a 50% reduction in the value of  $C_1$ , the value of ride comfort ( $W_z$ ) increases by about 9%.

- By increasing the value of  $C_2$ , the acceleration of the body, bogie, and wheel has decreased. Also, changes in body RMS acceleration and ride comfort have been minor.

- Increasing the mass of the body ( $M_1$ ), bogie ( $M_2$ ), and wheel ( $M_3$ ), respectively, reduces the RMS acceleration and vibration of the body, bogie, and wheel and vice versa. For example, with a decrease of 28%, 57%, and 71% of the value of  $M_3$  from the original value, the wheel RMS acceleration is increased by 26%, 80%, and 168%, respectively, and with an increase of 21%, 71%, and 157% % of the value of  $M_3$  from

the original value, the wheel RMS acceleration is decreased by 13%, 31%, and 50%, respectively.

It is noteworthy that the purpose of this paper is a comparative study of rolling stock parameters according to some references such as [20, 36, 47], however, if, a real Chinese CRH3 high-speed train with parameters of  $M_1=40 \times 10^3$  (kg),  $M_2=3200$  (kg),  $M_3=2400$  (kg),  $K_1=0.8 \times 10^6$  (N/m),  $K_2=2.08 \times 10^6$  (N/m),  $C_1=120 \times 10^3$  (Ns/m),  $C_2=100 \times 10^3$  (Ns/m) according to the reference [20] be considered, the value of ride comfort will be 2.07 ( $(W_z)_{\text{Body}} = 2.07$ ). The present model is proposed assuming the load crosses the track without irrigation and on a tangent.

## References

- [1]. Jiang, Y., et al., Influence of bridge parameters on monorail vehicle-bridge system—A research with multi-rigid body and multi-flexible body coupling theory and Park method. *Journal of Low Frequency Noise, Vibration and Active Control*. 0(0): p. 1461348420942355.
- [2]. Jiang, Y., et al., Intelligent batch process method for analyzing the effect of the suspension parameters on the vibration of the suspended monorail. *Advances in Mechanical Engineering*, 2020. 12(10): p. 1687814020966421.
- [3]. Song, Y., et al., Evaluating the Effect of Wheel Polygons on Dynamic Track Performance in High-Speed Railway Systems Using Co-Simulation Analysis. *Applied Sciences*, 2019. 9(19): p. 4165.
- [4]. Kumar, V. and R. Vikas, Investigation of vertical dynamic behavior and modelling of a typical Indian rail road vehicle through bond graph. *World Journal of Modelling and Simulation*, 2009. 5.
- [5]. Gao, M., et al., Dynamic modeling and experimental investigation of self-powered sensor nodes for freight rail transport. *Applied Energy*, 2020. 257: p. 113969.
- [6]. Ye, Y., et al., Rotary-scaling fine-tuning (RSFT) method for optimizing railway wheel profiles and its application to a locomotive. *Railway Engineering Science*, 2020. 28(2): p. 160-183.

- [7]. Chaar, N. and M. Berg, Simulation of vehicle-track interaction with flexible wheelsets, moving track models and field tests. *Vehicle System Dynamics*, 2006. 44(sup1): p. 921-931.
- [8]. Leblebici, A.S. and S. Türkay, Track Modelling and Control of a Railway Vehicle. *IFAC-PapersOnLine*, 2016. 49(21): p. 274-281.
- [9]. Abood, K.H.A. and R.A. Khan, Railway carriage simulation model to study the influence of vertical secondary suspension stiffness on ride comfort of railway carbody. *Proceedings of the Institution of Mechanical Engineers, Part C: Journal of Mechanical Engineering Science*, 2011. 225(6): p. 1349-1359.
- [10]. Nielsen, J.C.O. and A. Igeland, VERTICAL DYNAMIC INTERACTION BETWEEN TRAIN AND TRACK INFLUENCE OF WHEEL AND TRACK IMPERFECTIONS. *Journal of Sound and Vibration*, 1995. 187(5): p. 825-839.
- [11]. Graa, M., et al. Modeling and Simulation for Vertical Rail Vehicle Dynamic Vibration with Comfort Evaluation. 2015. Cham: Springer International Publishing.
- [12]. Serajian, R., Parameters' changing influence with different lateral stiffnesses on nonlinear analysis of hunting behavior of a bogie. *Journal of Measurements in Engineering*, 2013. 1(4), p. 195-206.
- [13]. Uyulan, C., et al., Dynamic Investigation of the Hunting Motion of a Railway Bogie in a Curved Track via Bifurcation Analysis. *Mathematical Problems in Engineering*, 2017. DOI: 10.1155/2017/8276245.
- [14]. Serajian, R., et al., Effects of bogie and body inertia on the nonlinear Wheel-set Hunting Recognized by the Hopf Bifurcation Theory, *International Journal of Automotive Engineering*, 2011, 1, p. 10.
- [15]. Anant, M., and Ahmadian, M., Nonlinear investigation of the effect of suspension parameters on the hunting stability of a railway truck, *Rail Conference*, 2006. P. 327-336.
- [16]. Yin, X., X. Wei, and H. Zheng, Applying System Dynamics of Discrete Supported Track to Analyze the Rail Corrugation Causation on Curved Urban Railway Tracks. *Discrete Dynamics in Nature and Society*, 2021. 2021: p. 9958163.
- [17]. Deng, C., et al., Analysis of the consistency of the Sperling index for rail vehicles based on different algorithms. *Vehicle System Dynamics*, 2021. 59(2): p. 313-330.
- [18]. Wu, J. and Y. Qiu, Modelling and ride comfort analysis of a coupled track-train-seat-human model with lateral, vertical and roll vibrations. *Vehicle System Dynamics*, 2021: p. 1-36.
- [19]. Cheng xiang, Ji., et al., Realistic fatigue damage assessment of a high-speed train bogie frame by damage consistency load spectra based on measured field load. *Measurement*, 2020. 166, p. 108164.
- [20]. Lei, X., *High Speed Railway Track Dynamics*. 1 ed. 2017: Springer, Singapore.
- [21]. Azrah, K., et al., The study of whole-body vibration effects on the passenger's comfort commuting in Tehran metro system. *Journal of Health and Safety at Work*, 2016. 6(1): p. 81-94.
- [22]. Keykaous, A., et al., Assessment of Metro Passengers' Convenience While Sitting and Standing in Confrontation with Whole-Body Vibration. *International Journal of Occupational Hygiene*, 2015. 6(4).
- [23]. Sun, J., et al., An investigation into evaluation methods for ride comfort of railway vehicles in the case of carbody hunting instability. *Proceedings of the Institution of Mechanical Engineers, Part F: Journal of Rail and Rapid Transit*, 2021. 235(5): p. 586-597.
- [24]. ISO, I., 2631-1: Mechanical vibration and shock-evaluation of human exposure to whole-body vibration-Part 1: General requirements. Geneva, Switzerland: ISO, 1997.
- [25]. Standardization, I.O.f., *Evaluation of Human Exposure to Whole-body Vibration*. 1985: ISO.



- [26]. Institution, B.S., Guide to measurement and evaluation of human exposure to whole-body mechanical vibration and repeated shock. 1999: British Standards Institution.
- [27]. Helbig, W. and E. Sperling, Verfahren zur beurteilung der laufeigenschaften von eisenbahnwagen (Process for the evaluation of the running behavior of railway vehicles). *Organ Für Die Fortschr. Des Eisenb*, 1941. 96: p. 177-187.
- [28]. Sperling, E. and C. Betzhold, Beitrag zur beurteilung des fahrkomforts in schienenfahrzeugen. *Glaser's Annalen*, 1956. 80: p. 314-320.
- [29]. Railways, I.U.o., UIC Code 513, R: Guidelines for Evaluating Passenger Comfort in Relation to Vibration in Railway Vehicles. 1995: International Union of Railways.
- [30]. CEN, E., 12299: Railway applications—Ride comfort for passengers—Measurement and evaluation. Google Scholar, 2009.
- [31]. Dumitriu, M. and D.I. Stănică, Study on the Evaluation Methods of the Vertical Ride Comfort of Railway Vehicle—Mean Comfort Method and Sperling's Method. *Applied Sciences*, 2021. 11(9): p. 3953.
- [32]. Sadeghi, J., S. Rabiee, and A. Khajehdezfuly, Effect of Rail Irregularities on Ride Comfort of Train Moving Over Ballast-Less Tracks. *International Journal of Structural Stability and Dynamics*, 2019. 19(06): p. 1950060.
- [33]. Esveld, C., Modern railway track (The Netherlands: MRT-Productions 2001). Google Scholar.
- [34]. Zhou, B., X.-Y. Xie, and Y. Yang, Simulation of wave propagation of floating slab track-tunnel-soil system by 2D theoretical model. *International Journal of Structural Stability and Dynamics*, 2014. 14(01): p. 1350051.
- [35]. Kumar, V., V. Rastogi, and P. Pathak, Simulation for whole-body vibration to assess ride comfort of a low-medium speed railway vehicle. *SIMULATION*, 2017. 93(3): p. 225-236.
- [36]. Karthik Hebbar A, P.C., Srinidhi Ramachandracharya, Analytical Modeling of Railway Suspension System using MATLAB Simulink. *International Journal of Recent Technology and Engineering (IJRTE)*, 2019. 8(1S2): p. 164-168.
- [37]. Real, J., et al., Modelling vibrations caused by tram movement on slab track line. *Mathematical and Computer Modelling*, 2011. 54(1–2): P. 280-291.
- [38]. Galvín, P., et al., Vibrations induced by HST passage on ballast and non-ballast tracks. *Soil Dynamics and Earthquake Engineering*, 2010. 30(9): P. 862-873.
- [39]. Gong, D., J. Zhou, and W. Sun, Influence of under-chassis-suspended equipment on high-speed EMU trains and the design of suspension parameters. *Proceedings of the Institution of Mechanical Engineers, Part F: Journal of Rail and Rapid Transit*, 2016. 230(8): p. 1790-1802.
- [40]. Sun, Y., et al., A New Vibration Absorber Design for Under-Chassis Device of a High-Speed Train. *Shock and Vibration*, 2017. 2017: p. 1523508.
- [41]. Ling, L., et al., Integration of car-body flexibility into train-track coupling system dynamics analysis. *Vehicle System Dynamics*, 2018. 56(4): p. 485-505.
- [42]. Mpofo, I.A.D.a.K., Vibration Analysis and Control in the Rail Car System Using PID Controls, in *Noise and Vibration Control - From Theory to Practice*. 2019, IntechOpen. p. 1-17.
- [43]. Kouroussis, G., D.P. Connolly, and O. Verlinden, Railway-induced ground vibrations – a review of vehicle effects. *International Journal of Rail Transportation*, 2014. 2(2): p. 69-110.
- [44]. Kouroussis, G., et al., The effect of railway local irregularities on ground vibration. *Transportation Research Part D: Transport and Environment*, 2015. 39: p. 17-30.
- [45]. Koç, M.A. and İ. Esen, Modelling and analysis of vehicle-structure-road coupled interaction considering structural flexibility, vehicle parameters and road roughness. *Journal of Mechanical*

Science and Technology, 2017. 31(5): p. 2057-2074.

[46]. Sharma, R., Parametric analysis of rail vehicle parameters influencing ride behavior. International Journal of Engineering, Science and Technology, 2011. 3(8): p. 54-65.

[47]. Koh, C. G., et al., Moving element method for train-track dynamics. International Journal for Numerical Methods in Engineering, 2003. 56(11): p. 1549–1567.